

# Abrupt changes and hysteretic behavior of $90^\circ$ domains in epitaxial ferroelectric thin films with misfit dislocations

A. Yu. Emelyanov and N. A. Pertsev

*A. F. Ioffe Physico-Technical Institute, Russian Academy of Sciences, 194021 St. Petersburg, Russia*

(Received 28 April 2003; revised manuscript received 13 October 2003; published 22 December 2003)

The influence of misfit dislocations on the statics and dynamics of  $90^\circ$  domains (twins) in epitaxial thin films is studied theoretically. The misfit dislocations create additional potential barriers, which hinder the movements of domain walls along the film/substrate interface. For ferroelastic  $90^\circ$  walls, these barriers are considerable because an *elastic interaction* exists between  $90^\circ$  domains and misfit dislocations owing to the coupling of the dislocation stresses to the spontaneous strains generated at the proper or improper ferroelastic phase transition. The energy of elastic interaction is evaluated for a single  $90^\circ$  domain embedded into a tetragonal film containing a periodic array of edge misfit dislocations. On this basis, the equilibrium width of a single embedded  $90^\circ$  domain is calculated as a function of the misfit strain in the film/substrate system. It is found that, at some threshold values of the misfit strain, the gradual variation of the domain width is interrupted by steplike changes. The evolution of the  $90^\circ$  domain pattern during the polarization switching in ferroelectric films with misfit dislocations is analyzed in detail. The calculations show that the electric-field-induced growth of an embedded  $90^\circ$  domain involves three different stages. Remarkably, at some critical value of the applied electric field, one of the  $90^\circ$  domain walls jumps over the neighboring misfit dislocation, which is accompanied by abrupt changes of the domain width and position in the film. The steplike movements of  $90^\circ$  domain walls over the misfit dislocations are proposed as a possible microscopic mechanism of the *Barkhausen effect* occurring in ferroelectric thin films during the polarization reversal. The hysteretic behavior of  $90^\circ$  domains at the cyclic variation of an applied electric field is also demonstrated.

DOI: 10.1103/PhysRevB.68.214103

PACS number(s): 77.80.Dj, 77.55.+f

## I. INTRODUCTION

The presence of misfit dislocations is a characteristic structural feature of epitaxial thin films grown on dissimilar substrates.<sup>1</sup> These linear defects provide a partial relaxation of lattice strains in the films exceeding a critical thickness.<sup>2</sup> In ferroelastic thin films, the formation of elastic domains (twins) represents an additional microscopic mechanism of the strain relaxation.<sup>3</sup> As observed experimentally,<sup>4–19</sup> this relaxation mechanism often operates in epitaxial films of perovskite ferroelectrics, which are improper ferroelastics. The generation of misfit dislocations in perovskite films<sup>6,15,17,20–26</sup> is believed to occur mainly at the growth temperature  $T_g$ ,<sup>14,22</sup> because the dislocation glide must be suppressed at  $T \ll T_g \sim 700^\circ\text{C}$  due to the relatively high Peierls barriers in perovskites. In contrast, the domain formation takes place well below  $T_g$  at a phase transition temperature  $T_c$ , and the ferroelastic ( $90^\circ$ ) domain walls remain mobile down to room temperature.<sup>27,28</sup> Thus, the statics and dynamics of  $90^\circ$  domains in ferroelectric thin films may be affected considerably by the interaction with (immobile) misfit dislocations.

The effect of misfit dislocations on the domain structures of epitaxial perovskite films was first studied theoretically by Speck and Pompe.<sup>29</sup> In their fundamental paper, it was shown that arrays of misfit dislocations screen the film from the substrate potential so that an effective substrate lattice parameter  $b^*$  must be used to predict equilibrium domain configurations in real epitaxial systems. The theory of Speck and Pompe, however, was developed in a continuum approximation, which replaces the actual arrays of *discrete*

misfit dislocations by continuum distributions of fictitious dislocations with infinitesimal Burgers vectors. This simple approximation provides a correct description of the “average” effect of misfit dislocations on the *statics* of domain patterns. For relatively thick films, where the equilibrium domain widths are much larger than the dislocation spacing, the accuracy of this approximation is quite good (see Sec. III). On the other hand, the continuum approach cannot properly describe the influence of misfit dislocations on the *dynamics* of ferroelastic and ferroelectric domains. This approach allows for a relaxation of mean mechanical stresses in the film but neglects highly inhomogeneous stress fields, which are induced by the dislocation arrays near the film/substrate interface. These fields create additional potential barriers, which hinder the movements of ferroelastic domain walls in the film plane.

The discreteness of misfit-dislocation arrays can be taken into account by using the actual stress fields of straight dislocations in the theoretical calculations. Recently, we derived an integral expression for the energy of elastic interaction between  $90^\circ$  domain configurations and discrete misfit dislocations in an epitaxial film.<sup>30</sup> This expression was used to calculate the interaction force for a  $90^\circ$  wall inclined at  $45^\circ$  to the surfaces of a tetragonal thin film. It was shown that the misfit dislocations with the Burgers vector orthogonal to the film/substrate interface create substantial pinning forces for the domain wall. The critical electric field, which should be applied to a ferroelectric film in order to overcome the pinning of  $90^\circ$  walls by these misfit dislocations, may be as large as  $10^7$  V/m.<sup>30</sup>

In this paper, we investigate the statics and dynamics of

90° domains embedded into a tetragonal film containing a periodic array of edge misfit dislocations. We focus on the most important type of domain pattern, which consists of dissimilar domains with the tetragonal  $c$  axis orthogonal and parallel to the interface. These  $c$  and  $a$  domains are separated by 90° walls inclined at about 45° to the interface, which are widely observed experimentally.<sup>4,5,9,11</sup> The interaction energy of an embedded domain with the dislocations having the in-plane orientation of the Burgers vector is evaluated in a linear isotropic approximation (Sec. II). The screening of the dislocation stress field by the film free surface is taken into account, as well as the finite thickness of 90° walls, which is a typical feature of ferroelastic domain boundaries.<sup>31–34</sup> The calculated interaction energy is used to study the energetics of an isolated 90° domain in the epitaxial film grown on a dissimilar cubic substrate (Sec. III). The energetically most favorable position of the embedded domain with respect to the dislocation array is determined, and the equilibrium domain width is calculated as a function of the misfit strain in the film/substrate system. In Sec. IV, the growth of the ferroelectric 90° domain in a gradually increasing external electric field is described. The results of theoretical calculations are discussed in Sec. V. It should be emphasized that these results may be useful for theoretical studies of the influence of misfit dislocations on the physical properties of ferroelectric thin films, which are important for their applications in microelectronic and micromechanical devices.

## II. ELASTIC INTERACTION BETWEEN FERROELASTIC DOMAINS AND MISFIT DISLOCATIONS

Proper and improper ferroelastic phase transitions in crystals lead to changes of the sizes and shape of the unit cell.<sup>34</sup> When the crystal is free of mechanical stresses, these changes are completely determined by the *spontaneous* (transformation) strains  $S_{ij}^0$  ( $i, j = 1, 2, 3$ ) of the lattice. In the presence of the sources of internal stresses (or external mechanical loading), the *total* lattice strains  $S_{ij}^t(\mathbf{r})$  differ from the spontaneous strains  $S_{ij}^0(\mathbf{r})$  since the crystal lattice is also deformed *elastically*. Moreover, the mechanical stresses  $\sigma_{ij}$  may produce a work during the development of excess lattice strains at the phase transition. A nonzero magnitude of this work indicates the existence of an elastic interaction between the ferroelastic phase and a source of stress.

The interaction energy  $W_{\text{int}}$  may be evaluated in the approximation of the linear theory of elasticity.<sup>35</sup> Using Colonnetti's theorem, it can be shown that the spontaneous strains  $S_{ij}^0(\mathbf{r})$  only must be taken into account in the calculation of the work produced by stresses  $\sigma_{ij}$ . Defining the tensor of spontaneous strains  $S_{ij}^0(\mathbf{r})$  in the crystal reference frame common for all elastic domains, we obtain

$$W_{\text{int}} = - \int_V S_{ij}^0(\mathbf{r}) \sigma_{ij}(\mathbf{r}) dV, \quad (1)$$

where the integration is carried out over the volume  $V$  of ferroelastic phase, and the summation over repeated indices should be carried out. The strains  $S_{ij}^0(\mathbf{r})$  involved in Eq. (1) take different values in dissimilar domains and vary in a

continuous manner across ferroelastic domain walls having a finite thickness. Therefore, the interaction energy  $W_{\text{int}}$  depends on the type and geometry of domain structure formed in the ferroelastic phase.

By definition, ferroelastic (twin) walls separate domains, which differ by at least one component  $S_{kl}^0$  of the strain tensor  $S_{ij}^0(\mathbf{r})$ . Accordingly, translational displacements of these walls in a stress field with  $\sigma_{kl} \neq 0$  will change the interaction energy even in the case when the field is homogeneous. The coupling between  $S_{kl}^0$  and  $\sigma_{kl}$  represents the most important term in Eq. (1) since it gives rise to the thermodynamic force acting on domain walls, which is proportional to the stress  $\sigma_{kl}$  itself. The existence of other contributions to the interaction energy is due to local changes of the strain components  $S_{ij}^0(\mathbf{r})$  inside domain walls.<sup>32,33</sup> These terms are less important because the associated forces are governed by the stress gradients  $\nabla \sigma_{ij}(\mathbf{r})$  only. Restricting our analysis to the stress sources with  $\sigma_{kl} \neq 0$ , we can retain in Eq. (1) only the leading term  $S_{kl}^0 \sigma_{kl}$  and ignore the other terms in the first approximation.

To evaluate the interaction energy  $W_{\text{int}}$  quantitatively, it is necessary to specify the strain field  $S_{kl}^0(\mathbf{r})$  in a polydomain (twinned) crystal. In the linear approximation, which neglects the influence of mechanical stresses on the order parameters, the homogeneous spontaneous strains characterizing the inner regions of domains may be set equal to the strains  $S_{kl}^0$  developing in a stress-free single-domain crystal. The variation of strains  $S_{kl}^0(\mathbf{r})$  inside domain walls should match in a continuous manner the plateau values attained within the neighboring domains. Using a simple model introduced in Ref. 36, we may assume a linear variation of  $S_{kl}^0$  inside domain-wall regions with an effective thickness  $2w$ . As for the geometry of domain pattern, we shall suppose that ferroelastic domain boundaries are flat and oriented along specific planes that determine the energetically most favorable orientations of domain walls in a stress-free crystal.<sup>37</sup> Accordingly, the curvature of domain boundaries, which may be induced by inhomogeneous extraneous stresses, will be neglected in our calculations. The approximation of planar boundaries is justified by the fact that curved twin walls are the sources of long-range stress fields and so energetically strongly unfavorable.<sup>38</sup>

We now focus on the case of a (001)-oriented thin film experiencing a cubic to tetragonal phase transition. In the crystallographic frame  $(x_1, x_2, x_3)$  with the  $x_3$  axis orthogonal to the film surfaces (see Fig. 1), the nonzero spontaneous strains inside the  $c$  domain are equal to  $S_{11}^0 = S_{22}^0 = (a - a_0)/a_0 = S_a^0$  and  $S_{33}^0 = (c - a_0)/a_0 = S_c^0$ . (Here  $a$  and  $c > a$  are the lattice parameters of a stress-free tetragonal phase, and  $a_0$  is the lattice constant of the prototypic cubic state extrapolated to a given temperature  $T < T_c$ .) In the  $a$  domain with the tetragonal axis parallel to the  $x_1$  axis, the spontaneous strains become  $S_{11}^0 = S_c^0$  and  $S_{22}^0 = S_{33}^0 = S_a^0$ . It can be seen that the strain components  $S_{11}^0$  and  $S_{33}^0$  change on crossing the boundary between  $c$  and  $a$  domains. Accordingly, we shall assume that, inside the  $c/a$  domain wall,  $S_{11}^0$  and  $S_{33}^0$

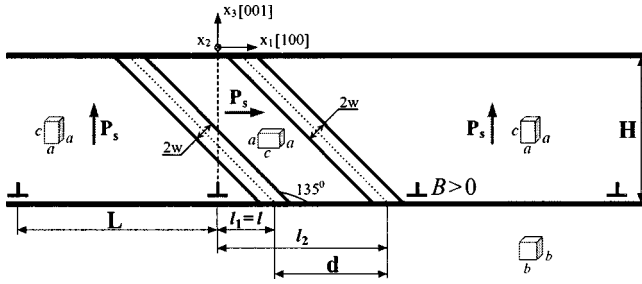


FIG. 1. Domain  $c/a/c$  configuration in a tetragonal epitaxial film containing two periodic arrays of edge misfit dislocations. The embedded  $a$  domain of the size  $d$  is bounded by  $90^\circ$  walls having the thickness  $2w$ . Symbols  $\perp$  denote edge dislocations with the Burgers vector  $\mathbf{B}_1$  distributed along the interface with the period  $L$ . The dislocation array with the Burgers vector  $\mathbf{B}_2$  parallel to the twinning axis  $x_2$  is not depicted. The vectors  $\mathbf{P}_s$  show the spontaneous polarizations of ferroelectric domains.

vary linearly between the values of  $S_a^0$  and  $S_c^0$ . In contrast, the component  $S_{22}^0$  may be taken to be uniform in the wall region.

Consider first the  $c/a/c$  domain configuration, which consists of the single  $a$  domain embedded into the otherwise  $c$ -domain film. For our purposes, it is convenient to count the interaction energy  $W_{\text{int}}$  characterizing a polydomain state from the value calculated for a reference single-domain state. Then from Eq. (1) we obtain the following integral expression for the interaction energy  $\Delta W_{\text{int}}^a = W_{\text{int}}^{c/a/c} - W_{\text{int}}^c$  of the embedded  $a$  domain:

$$\begin{aligned} \Delta W_{\text{int}}^a = & -\frac{1}{2}(S_c^0 - S_a^0) \int_{-\infty}^{\infty} dx_2 \int_{-H}^0 dx_3 \\ & \times \left\{ \int_{l_1 - \sqrt{2}w - H - x_3}^{l_1 + \sqrt{2}w - H - x_3} \left[ 1 + \frac{(x_1 + x_3 - l_1 + H)}{\sqrt{2}w} \right] \right. \\ & \times (\sigma_{11} - \sigma_{33}) dx_1 + \int_{l_1 + \sqrt{2}w - H - x_3}^{l_2 - \sqrt{2}w - H - x_3} 2(\sigma_{11} - \sigma_{33}) dx_1 \\ & + \int_{l_2 - \sqrt{2}w - H - x_3}^{l_2 + \sqrt{2}w - H - x_3} \left[ 1 - \frac{(x_1 + x_3 - l_2 + H)}{\sqrt{2}w} \right] \\ & \left. \times (\sigma_{11} - \sigma_{33}) dx_1 \right\}, \end{aligned} \quad (2)$$

where  $\sigma_{ij} = \sigma_{ij}(x_1, x_2, x_3)$  are the stresses created by misfit dislocations (or other defects);  $l_1$  and  $l_2$  denote the positions of domain boundaries in the film,  $H$  is the film thickness, and it is assumed that the  $c/a$  walls are parallel to the (101) plane of the prototypic cubic phase (see Fig. 1). It can be easily shown that the interaction energy  $\Delta W_{\text{int}}^c = W_{\text{int}}^{a/c/a} - W_{\text{int}}^a$  of the  $c$  domain embedded into the  $a$ -domain film differs from  $\Delta W_{\text{int}}^a$  only by the opposite sign.

When the stress field  $\sigma_{ij}(x_1, x_2, x_3)$  is known, Eq. (2) makes it possible to evaluate the energy of elastic interaction as a function of the domain position in the film and the domain width  $d = l_2 - l_1$ . The differentiation of Eq. (2) with

respect to the parameters  $l_1$  and  $l_2$  also enables a calculation of the in-plane thermodynamic forces  $F_{\text{int}}^{(\alpha)} = -\partial \Delta W_{\text{int}} / \partial l_\alpha$  ( $\alpha = 1, 2$ ) acting on the  $c/a$  and  $a/c$  domain boundaries in the presence of mechanical stresses  $\sigma_{ij}$ . It can be seen that even a homogeneous stress field  $\sigma_{ij}$  may exert a nonzero force on these ferroelastic  $90^\circ$  walls.

The stresses  $\sigma_{ij}(x_1, x_2, x_3)$  created by misfit dislocations in a thin film depend on the geometry of the dislocation pattern and the orientation of the Burgers vectors with respect to the dislocation lines. For a perovskite film grown in the paraelectric cubic state on a (001)-oriented cubic substrate, the formation of two arrays of mutually orthogonal straight edge dislocations parallel to the [010] and [100] crystallographic axes is expected.<sup>29</sup> We shall assume, for simplicity, that these dislocations are distributed along the film/substrate interface with the same spacing  $L$  and lie exactly on this interface. Since only the in-plane components of the dislocation Burgers vectors  $\mathbf{B}_1$  and  $\mathbf{B}_2$  provide the relaxation of misfit strain in the epitaxial system, these vectors may be taken to be parallel to the [100] and [010] axes, respectively. Then the analytic expressions derived in Ref. 39 for the stresses created by a straight edge dislocation in an isotropic elastic half-space can be used in our calculations, if we neglect the anisotropy and inhomogeneity of elastic properties of the film/substrate system. The stress field of an infinite periodic dislocation array can be easily found by summing the stresses of individual dislocations.<sup>35</sup> Substituting the calculated total stresses  $\sigma_{ij}(x_1, x_2, x_3)$  created by two dislocation arrays into Eq. (2) and performing the integration, we finally obtain the interaction energy of the  $a$  domain as

$$\begin{aligned} \Delta W_{\text{int}}^a = & \frac{GB(S_c^0 - S_a^0)}{2(1-\nu)} \left\{ \int_0^d \left[ J\left(\frac{x+l+\sqrt{2}w}{L}, \frac{H}{L}\right) \right. \right. \\ & + J\left(\frac{x+l-\sqrt{2}w}{L}, \frac{H}{L}\right) \left. \right] dx + \int_{-\sqrt{2}w}^{\sqrt{2}w} \frac{x}{\sqrt{2}w} \left[ J\left(\frac{x+l}{L}, \frac{H}{L}\right) \right. \\ & - J\left(\frac{x+d+l}{L}, \frac{H}{L}\right) \left. \right] dx \mp \frac{H^2}{\pi\sqrt{2}w} \left[ I\left(\frac{l+\sqrt{2}w}{L}, \frac{H}{L}\right) \right. \\ & - I\left(\frac{l-\sqrt{2}w}{L}, \frac{H}{L}\right) - I\left(\frac{d+l+\sqrt{2}w}{L}, \frac{H}{L}\right) \\ & \left. \left. + I\left(\frac{d+l-\sqrt{2}w}{L}, \frac{H}{L}\right) \right] - 4\nu \frac{dH}{L} \right\}, \end{aligned} \quad (3)$$

where  $G$  and  $\nu$  are the effective shear modulus and Poisson's ratio of the film/substrate system treated as an elastically isotropic and homogeneous half-space,  $B$  is the projection of the dislocation Burgers vector  $\mathbf{B}_1$  on the  $x_1$  axis (the projection of  $\mathbf{B}_2$  on the  $x_2$  axis is the same in the cube-on-cube epitaxy),  $l$  defines the position of the left domain boundary with respect to the misfit-dislocation array (see Fig. 1), and the interaction energy is given per unit domain length along the [010] axis. The upper and lower signs in the second line of Eq. (3) correspond to the two possible orientations of the boundaries of a  $90^\circ$  domain, i.e., those parallel to the crys-

tallographic planes (10 $\bar{1}$ ) and (101), respectively. The dimensionless functions  $J$  and  $I$  involved in Eq. (3) have the forms

$$J(x, y) = \frac{1}{4\pi} \ln \left[ \frac{\cosh(4\pi y) - \cos(2\pi x)}{1 - \cos(2\pi x)} \right] + \frac{y \sinh(4\pi y)}{\cosh(4\pi y) - \cos(2\pi x)} - 2\pi y^2 \frac{[\cosh(4\pi y) \cos(2\pi x) - 1]}{[\cosh(4\pi y) - \cos(2\pi x)]^2}, \quad (4)$$

$$I(x, y) = \arctan[\tan(\pi x) \coth(2\pi y)]. \quad (5)$$

Equations (3)–(5) will be used below to describe quantitatively the influence of misfit-dislocation arrays on the statics and dynamics of 90° domains in epitaxial films.

In conclusion of this section we emphasize that purely ferroelectric 180° domain walls interact with the misfit dislocations as well. The interaction force of elastic origin, however, is expected to be relatively weak since it is determined by the gradient  $\nabla \sigma_{ij}(\mathbf{r})$  of the dislocation stress field. To calculate the interaction force for an 180° domain wall, it is necessary to take into account the local changes of spontaneous strains inside the wall,<sup>33</sup> because the tensor  $S_{ij}^0$  is the same in both domains adjoining the 180° wall.

### III. STATICS OF 90° DOMAINS IN EPITAXIAL FILMS WITH PERIODIC DISLOCATION ARRAYS

Consider the energetics of the  $c/a/c$  and  $a/c/a$  domain configurations in tetragonal thin films with periodic arrays of misfit dislocations. The change  $\Delta U_a^{\text{md}}$  of the internal energy of an epitaxial system at the formation of the embedded  $a$  domain is defined by the sum of the domain self-energy  $\Delta W_s^a$  in a dislocation-free film and the interaction energy  $\Delta W_{\text{int}}^a$  of this domain with misfit dislocations. In the linear approximation, the energy  $\Delta W_s^a$  reduces to the sum of the elastic contribution and the energy of two 90° domain walls. For the  $a$  domain with boundaries of finite thickness  $2w$ , the self-energy  $\Delta W_s^a$  per unit domain length along the [010] axis has been calculated in Ref. 40 as

$$\Delta W_s^a = \frac{G(S_a - S_c)^2 H^4}{16\pi(1-\nu)w^2} \left\{ 2g\left(\frac{d}{2H}\right) + 2g\left(\frac{\sqrt{2}w}{H}\right) - g\left(\frac{d+2\sqrt{2}w}{2H}\right) - g\left(\frac{d-2\sqrt{2}w}{2H}\right) \right\} - \frac{2GH^2}{(1-\nu)}(1+\nu)S_a(S_a - S_c)\frac{d}{H} + 2\sqrt{2}\sigma H, \quad (6)$$

where  $S_a = (b-a)/a$ ,  $S_c = (b-c)/c$ ,  $b$  is the lattice parameter of a cubic substrate,  $\sigma$  is the 90°-wall energy per unit area, and the dimensionless function  $g$  is given by

$$g(x) = \left(8x^2 - \frac{14}{3}\right) \ln(1+x^2) - \frac{2}{3}x^4 \ln\left(1 + \frac{1}{x^2}\right) + \frac{16}{3}x(4-x^2)\arctan(x). \quad (7)$$

Using Eqs. (3) and (6) and taking into account that in real epitaxial systems  $S_a, S_c, S_a^0, S_c^0 \ll 1$ , we can represent the energy  $\Delta U_a^{\text{md}}$  in the following general form:

$$\Delta U_a^{\text{md}} = \sigma \frac{H^2}{H_0} \left\{ \frac{1}{4\pi} \left(\frac{H}{2w}\right)^2 Z\left(\frac{d}{H}, \frac{2w}{H}\right) - \frac{S_r}{S_r^0} \frac{d}{H} \right\} + \frac{\sigma BH}{(S_c^0 - S_a^0)H_0} Y\left(\frac{d}{H}, \frac{2w}{H}, \frac{L}{H}, \frac{l}{L}\right) + 2\sqrt{2}\sigma H, \quad (8)$$

where  $Z$  denotes the function given by the expression in the curly brackets in Eq. (6),  $Y$  is the expression in the curly brackets in Eq. (3) divided by  $2H$ ,  $H_0 = \sigma(1-\nu)/[G(S_a - S_c)^2]$  is the characteristic thickness for polydomain films,<sup>41</sup>  $S_r = (b-a)/(c-a)$  is the relative coherency strain<sup>42</sup> characterizing lattice misfits between the polydomain tetragonal film and the cubic substrate, and  $S_r^0 = 1/[2(1+\nu)]$  is the threshold value of  $S_r$ .<sup>41</sup> The energy  $\Delta U_c^{\text{md}}$  of the single  $c$  domain embedded into the  $a$ -type film is defined by the relation, which differs from Eq. (8) only by the replacement  $S_r/S_r^0 \rightarrow 2 - S_r/S_r^0$  and by the opposite sign of the second (interaction) term.

Equation (8) demonstrates that the normalized energy change  $\Delta U_a^{\text{md}}/(\sigma H)$  is a function of the relative domain size  $d/H$  and the domain position  $l/L$  with respect to the dislocation array. The domain energy also depends on the normalized wall thickness  $2w/H$  and the period  $L/H$  of the dislocation arrays, which may be regarded as constant quantities when analyzing the statics and dynamics of 90° domains. Besides,  $\Delta U_a^{\text{md}}/(\sigma H)$  depends on the standard parameters  $S_r/S_r^0$  and  $H/H_0$  of the film/substrate system and on the dimensionless ratio  $\beta = B/[H_0(S_c^0 - S_a^0)]$ , which characterizes the relative magnitude of the Burgers vector  $\mathbf{B}$ .<sup>43</sup>

The equilibrium domain size  $d^*$  and the energetically most favorable domain position  $l^*$  in the film can be calculated from the system of simultaneous equations  $\partial \Delta U_a^{\text{md}}/\partial d = 0$ , and  $\partial \Delta U_a^{\text{md}}/\partial l = 0$ , which follows from the minimization of the energy of  $c/a/c$  state. Therefore, the equilibrium values of  $d^*$  and  $l^*$  normalized by  $H_0$  appear to be functions of the parameters  $S_r/S_r^0, H/H_0, L/H, 2w/H$ , and  $\beta$  of the material system under consideration. Using Eqs. (3)–(7), we calculated numerically the dependence of  $d^*/H_0$  and  $l^*/H_0$  on the relative misfit strain  $S_r/S_r^0$  in the epitaxy at some representative values of the remaining parameters of the problem. Figure 2 shows this dependence determined for an epitaxial system with relatively sparse misfit dislocations ( $L=H=100H_0$ ). It can be seen that the variation of the domain size  $d^*$  with the misfit strain is marked by the presence of steplike changes, which interrupt the gradual domain growth. As demonstrated by Fig. 2(a), these abrupt changes take place when the domain size approaches the values  $d^*$

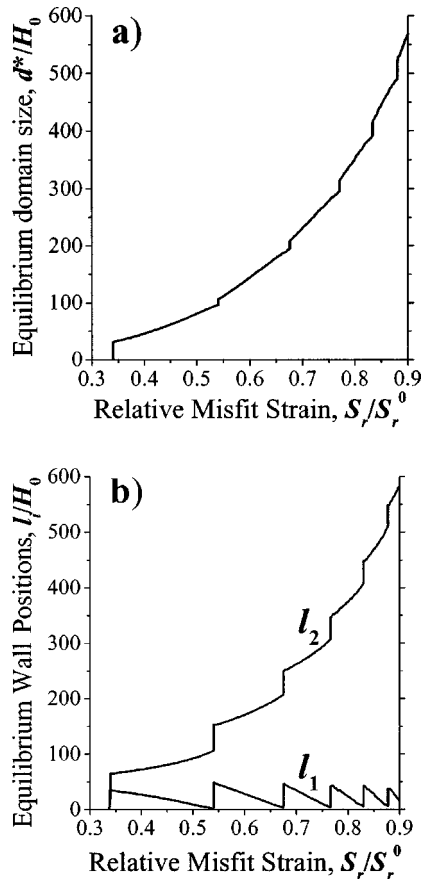


FIG. 2. Equilibrium geometry of the  $c/a/c$  domain pattern in a tetragonal film with two orthogonal arrays of misfit dislocations having Burgers vectors  $B_1 = B_2 = B > 0$ . Variations of the size  $d^*$  of the  $90^\circ$  domain and the equilibrium domain-wall positions  $l_1$  and  $l_2$  with the relative misfit strain  $S_r/S_r^0 = 2(1+\nu)(b-a)/(c-a)$  in the epitaxy are shown in (a) and (b), respectively. The film thickness  $H$  and the dislocation spacing  $L$  are taken to be  $H=L=100H_0$ . The  $90^\circ$  walls are parallel to the (101) plane, and their thickness is assumed to be  $2w=H_0$  here and below. Similar plots describe the equilibrium geometry of the  $a/c/a$  domain configuration in an epitaxial system with  $S_r/S_r^0 > 1$  and the dislocation arrays having  $B_1 = B_2 = B < 0$ . These plots can be obtained using the replacement  $S_r/S_r^0 \rightarrow 2 - S_r/S_r^0$ .

$=nL$  ( $n=1,2,3,4,\dots$ ). At corresponding threshold coherency strains, the  $90^\circ$  domain walls also shift considerably with respect to the misfit dislocations [see Fig. 2(b)].

The analysis of the calculated dependences  $d^*(S_r)$  and  $l^*(S_r)$  makes it possible to reveal the following peculiarities of the domain behavior in epitaxial films with misfit dislocations. Suppose that initially the strain parameter  $S_r/S_r^0 < 1$  has a certain value at which the size  $d^*(S_r/S_r^0)$  is smaller than the dislocation spacing  $L$ . If the Burgers vector is positive ( $B > 0$ ), the embedded  $a$  domain will be situated between two neighboring dislocations because this is the most energetically favorable position under given conditions. During the increase of the coherency strain  $S_r$ , which may be caused by the substrate bending or temperature variations, the  $90^\circ$  walls will first gradually approach the misfit dislocations. Owing to the elastic interaction with the dislocations,

the increase of domain size  $d^*$  slows down in this situation. Then, at some threshold value  $S_r^*$  of the coherency strain, a shift of the  $90^\circ$  domain as a whole into a new position becomes energetically favorable. Above this value, the domain center displaces along the interface by a distance of about  $L/2$  so that one of the neighboring dislocations turns to be located inside the embedded domain (at approximately equal distances from the junctions of  $90^\circ$  walls with the interface). The domain shift is accompanied by a steplike increase of the equilibrium domain size  $d^*$ . The direction of the shift is defined by the orientation of domain walls with respect to the substrate surface.

The next abrupt change of the  $90^\circ$  domain configuration occurs when the coherency strain  $S_r$  reaches a subsequent threshold value, at which the domain size  $d^*$  approaches  $2L$ . The shift of the domain center by about  $L/2$  in the film plane leads to the appearance of the second dislocation inside the  $a$  domain and to an abrupt increase of its size by some amount  $\Delta d^*$ . During the further variation of the coherency strain  $S_r$ , the gradual growth of the embedded domain also alternates with step-like changes of the equilibrium domain size. As the strain parameter  $S_r/S_r^0$  approaches unity, the difference between adjacent threshold values of  $S_r$  reduces due to the increasing steepness of smooth segments on the curve  $d^*(S_r)$  [see Fig. 2(a)].

When the misfit dislocations in an epitaxial system have negative Burgers vectors ( $B < 0$ ), it becomes energetically favorable to place the embedded  $a$  domain of a small size  $d^* < L$  in a different position, where one of the dislocations is situated inside the  $90^\circ$  domain at approximately equal distances from the wall junctions with the interface. In this case, an abrupt change of the domain configuration takes place when the boundaries of the growing domain approach the middle positions between neighboring misfit dislocations. Above the corresponding threshold value of  $S_r$ , the domain shifts by a distance of about  $L/2$  so that the number of dislocations inside it increases by unity. This shift is again accompanied by a steplike increase of the domain width.

The above theoretical results may be compared with the dependence  $d^*(S_r)$  calculated in the continuum approximation. The latter can be found by replacing the actual arrays of discrete dislocations by continuous distributions of dislocations with infinitesimal Burgers vectors.<sup>29</sup> The densities  $\rho_{21}$  and  $\rho_{12}$  of the dislocation distributions on the film/substrate interface should satisfy the relations  $\rho_{21} = B_1/L$  and  $\rho_{12} = B_2/L$ , which in our case of  $B_1 = B_2 = B$  reduce to the equality  $\rho_{21} = \rho_{12} = B/L$ . As shown by Speck and Pompe,<sup>29</sup> the introduction of such uniform dislocation distributions is equivalent to the replacement of the nominal substrate lattice parameter  $b$  by the effective parameter  $b^* = b(1 - B/L)$  in the basic expression  $S_r = (b - a)/(c - a)$  for the relative coherency strain. Therefore, the sought dependence  $d^*(S_r)$  can be calculated from the equation  $\partial \Delta W_s^a / \partial d = 0$ , where the self-energy  $\Delta W_s^a$  of the embedded  $a$  domain is given by Eq. (6) with the strain  $S_r$  replaced by  $S_r - \beta H_0/L$ .

Figures 3 and 4 demonstrate representative results of the rigorous calculations allowing for the discreteness of misfit dislocations in comparison with the dependences  $d^*(S_r)$  de-

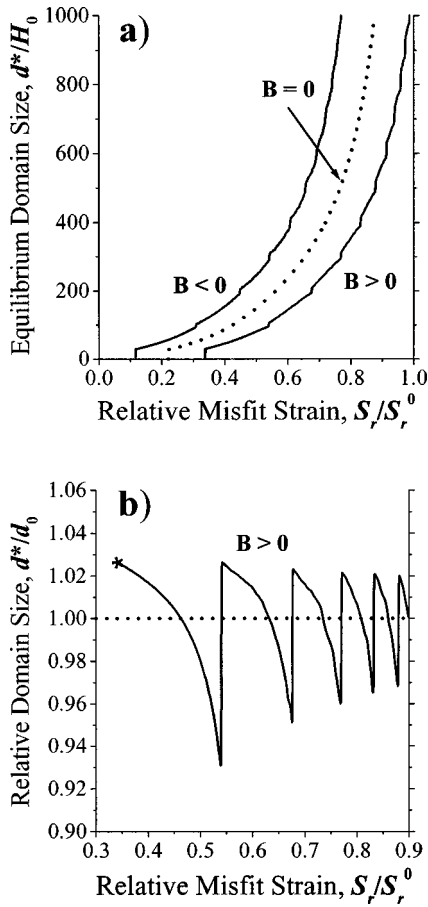


FIG. 3. Equilibrium size  $d^*$  of the embedded  $a$  domain as a function of the relative misfit strain  $S_r/S_r^0$  in the film/substrate system. The size  $d^*$  is normalized either by the characteristic film thickness  $H_0 = \sigma(1-\nu)/[G(S_c - S_a)^2]$  (a), or by the equilibrium domain width  $d_0$  calculated in the continuum approximation (b). The film thickness  $H$  and the dislocation spacing  $L$  are taken to be  $H=L=100H_0$ . The results obtained in the continuum approximation are shown in (a) only for a film without misfit dislocations ( $B=0$ ). Similar smooth curves plotted for films containing sparse misfit dislocations ( $L=H$ ) differ only slightly from the plots calculated from Eqs. (3)–(7).

terminated in the continuum approximation. Remarkably, even in the case of relatively sparse misfit dislocations ( $L=H$ ) the continuum model correctly describes the general trend of the domain-size variation with the coherency strain in an epitaxial system [Fig. 3(a)]. The error in the calculated domain width  $d^*$ , which is caused by the neglect of the discreteness of dislocations, does not exceed several per cent [see Fig. 3(b)]. When the distances between misfit dislocations are very large ( $L \gg H$ ), however, the deviations from the actual dependence  $d^*(S_r)$  become significant (Fig. 4). Moreover, the continuum model may lead to appreciable errors in the calculations of the stability range of a polydomain state on the strain scale, underestimating this range for films with sparse misfit dislocations. As can be seen from Fig. 4, e.g., the minimum coherency strain  $S_r$ , at which the  $c/a/c$  state becomes stable in an epitaxial film with misfit dislocations, is significantly smaller at  $L=10H$  than the value determined in the continuum approximation.

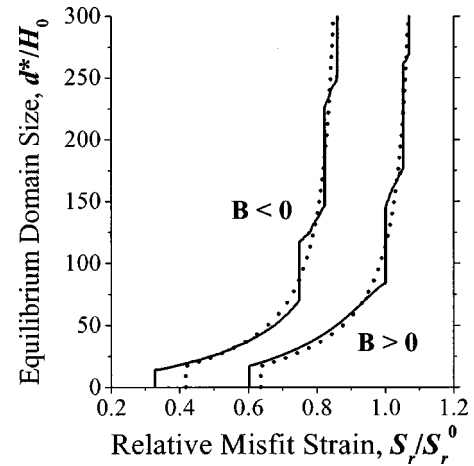


FIG. 4. Dependence of the normalized equilibrium size  $d^*/H_0$  of the  $a$  domain on the relative misfit strain  $S_r/S_r^0$  in the epitaxial system. The curves are plotted for a film with the thickness  $H=10H_0$  and the spacing between the misfit dislocations  $L=100H_0$ . The results obtained in the continuum approximation are shown by dotted lines.

#### IV. DYNAMICS OF A FERROELECTRIC $90^\circ$ DOMAIN IN ELECTRIC FIELD

In this section, we shall describe the influence of misfit dislocations on the evolution of  $90^\circ$  domain patterns in a ferroelectric film subjected to an external electric field. Our analysis will be restricted to relatively low-frequency fields, which are used in the measurements of polarization hysteresis loops in ferroelectrics. When the film is sandwiched between two continuous electrodes, as in a conventional plate-capacitor setup, the electric field intensity  $\mathbf{E}$  is predominantly oriented in the film-thickness direction. Therefore, the applied field interacts mainly with the out-of-plane spontaneous polarization  $\mathbf{P}_s$  existing in the  $c$  domains. Owing to this interaction, the width of a uniformly polarized  $c$  domain tends to increase or decrease after the application of electric field. In the absence of misfit dislocations, the embedded  $90^\circ$  domain in the  $c/a/c$  and  $a/c/a$  patterns will simply grow or shrink gradually, following temporal variations of the field intensity  $\mathbf{E}(t)$ . As will be shown below, the behavior of  $90^\circ$  domains may change markedly in epitaxial systems containing the misfit dislocations.

Consider as a representative example the dynamics of the  $a/c/a$  domain configuration, where the polarization vector  $\mathbf{P}_s$  in the  $c$  domain is oriented along the applied field. In this situation, the increase of the field intensity  $\mathbf{E}$  should lead to the growth of the embedded  $c$  domain. To quantify this process, we can employ the procedure proposed earlier in Ref. 44, where the effect of electric field on the energetics of  $90^\circ$  domains was studied for films without misfit dislocations. It was found that, in the linear approximation, the presence of a potential difference  $\Delta V$  between the top and bottom electrodes is equivalent to a change of the strain parameter  $S_r/S_r^0$  by a value  $\pm E/E_0$ , where  $E = \Delta V/H$ , and  $E_0 = G(S_a - S_c)^2/[(1-\nu)P_s]$  is the characteristic electric field introduced for a polydomain film. Then from Eq. (8) it follows that the field-induced variations of the equilibrium domain

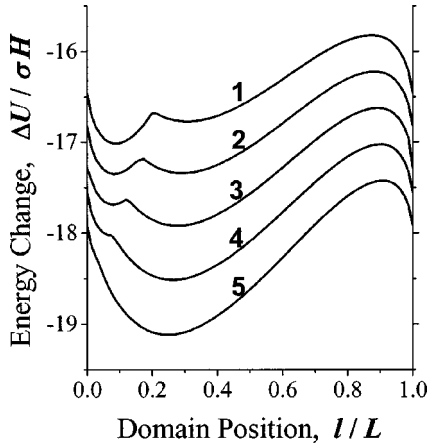


FIG. 5. Energy  $\Delta U_c^{\text{md}}$  of the  $a/c/a$  structure as a function of the domain position  $l$  with respect to the misfit-dislocation array. The film thickness equals  $H=10H_0$ , and the spacing between the misfit dislocations with the Burgers vectors  $B_1=B_2=B<0$  is assumed to be  $L=100H_0$ . Curves 1–5 are plotted at the following values of the relative misfit strain  $S_r/S_r^0$ : 1.006 (1), 1.002 (2), 0.998 (3), 0.994 (4), and 0.990 (5). For  $\text{PbTiO}_3$  films at room temperature, the reduction of  $S_r/S_r^0$  by a value of 0.004 corresponds to an increase of the electric field  $E$  parallel to the polarization  $\mathbf{P}_s$  in the  $c$  domain by  $\Delta E \approx 8 \times 10^5$  V/m.

width  $d^*(E)$  and position  $l^*(E)$  can be found using the dependences  $d^*(S_r)$  and  $l^*(S_r)$  calculated in Sec. III.

In order to determine the evolution of the  $a/c/a$  domain structure in an increasing electric field, we shall analyze the dependence of the energy change  $\Delta U_c^{\text{md}}$  of an epitaxial system on the in-plane position  $l$  of the  $c$  domain at a fixed coherency strain  $S_r$  in the epitaxy. Since according to Eqs. (3) and (8) the energy  $\Delta U_c^{\text{md}}$  is a periodic function of the relative domain position  $l/L$  with respect to the dislocation array, it is sufficient to calculate  $\Delta U_c^{\text{md}}$  in the range  $0 < l/L < 1$ . In the course of these calculations, an optimum domain size  $d_{\text{op}}(l/L)$  must be found from the equation  $\partial \Delta U_c^{\text{md}} / \partial d = 0$  and then substituted back into Eq. (8) to find the minimum domain energy  $\Delta U_c^{\text{md}}(l/L)$  at each given value of  $l/L$ . Performing necessary numerical calculations, we determined the dependence  $\Delta U_c^{\text{md}}(l/L)$  for several slightly different values of the coherency strain  $S_r$  (see Fig. 5).

When discussing our theoretical results, we shall suppose that the relative coherency strain in an epitaxial system has the value  $S_r = 1.006S_r^0$ , which corresponds to curve 1 in Fig. 5. The potential relief  $\Delta U_c^{\text{md}}(l/L)$  described by this curve involves two minima separated by a potential barrier so that it has the form of a double-well potential. Since at the above value of  $S_r$  and the chosen sign of the dislocation Burgers vectors ( $B < 0$ ) the left minimum is deeper than the right one, it is energetically favorable to embed the  $c$  domain having a small size  $d^* < L$  between two neighboring misfit dislocations ( $l^* > d^*$ ), as shown in Fig. 6(a). The subsequent application of an electric field and the increase of its intensity  $E$  will lead to the growth of the embedded domain. This process can be divided into three different stages.

During the first stage of the process, a gradual increase of

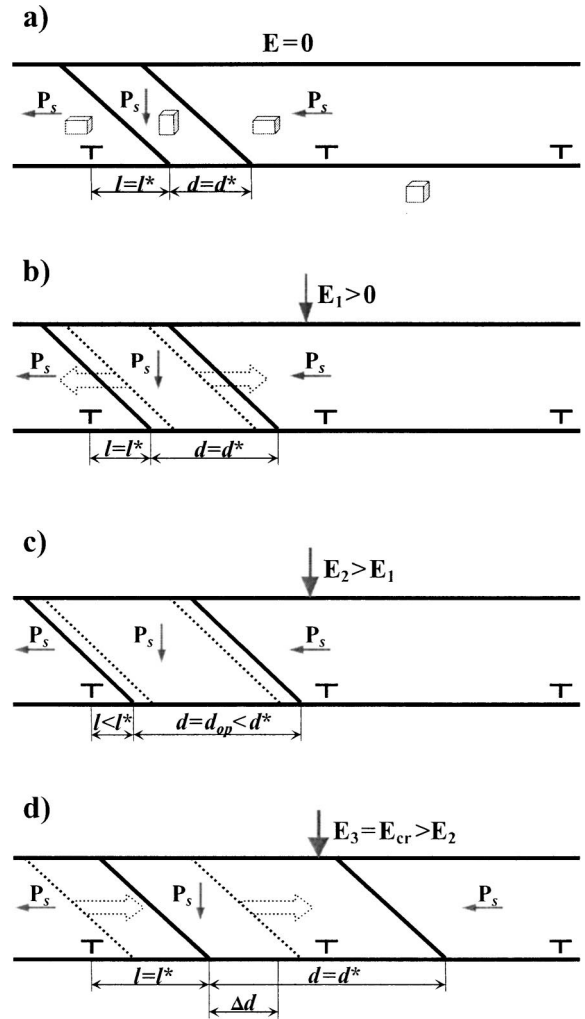


FIG. 6. Electric-field-induced evolution of the  $a/c/a$  domain structure in a ferroelectric film containing edge misfit dislocations: (a) initial  $90^\circ$  structure with the  $c$  domain embedded between two neighboring dislocations; (b) gradual expansion of the stable  $c$  domain under the action of increasing electric field  $\mathbf{E}$ ; (c) metastable state of the  $90^\circ$  domain clamped by the dislocations in a strong field; (d) abrupt change of the domain pattern caused by the jump of the right  $90^\circ$  wall over the neighboring misfit dislocation.

the equilibrium domain width  $d^* = d^*(S_r/S_r^0 - E/E_0)$  takes place, being similar to the initial smooth part of the curves shown in Fig. 4. This stage ends when the field intensity reaches a threshold value of  $E_{\text{th}} \approx 0.004E_0$ , at which the two minima of the energy  $\Delta U_c^{\text{md}}(l/L)$  become equal in depth. (At this field, the effective strain parameter  $S_r/S_r^0 - E/E_0$  reduces down to a value of 1.002 represented by curve 2 in Fig. 5.) At higher electric fields, it is energetically favorable to shift the  $c$  domain to another position  $l$ , which corresponds to the right minimum of the function  $\Delta U_c^{\text{md}}(l/L)$ . In this position, the domain contains one of the misfit dislocations since its equilibrium size  $d^*$  is larger than the dislocation spacing  $L$ . However, the domain shift is impeded by a potential barrier separating the two minima. Hence the  $90^\circ$  domain remains in a metastable state between the neighboring dislocations, growing only slightly with the increase of

the field intensity  $E$  [Fig. 6(c)]. At this second stage of the process, the domain width  $d_{\text{op}}$  differs from the equilibrium domain size  $d^*$  corresponding to the given value of the parameter  $S_r/S_r^0 - E/E_0$ . When the field intensity reaches the critical magnitude  $E_{\text{cr}} \approx 0.012E_0$ , the potential barrier between two energy minima disappears (curve 4 in Fig. 5). This leads to a “jump” of the right  $90^\circ$  wall over the misfit dislocation [Fig. 6(d)], which is accompanied by a shift of the domain center and the steplike increase  $\Delta d = d^* - d_{\text{op}}$  of the domain width (third stage of domain growth).

During the further rise of electric field, the above three-stage evolution of the  $a/c/a$  domain structure repeats. As soon as the field intensity reaches the next critical value, the right  $90^\circ$  wall leaps over the neighboring misfit dislocation again, and the number of dislocations inside the  $c$  domain increases by unity. Since the resulting abrupt change of the domain size is accompanied by a steplike increase in the mean polarization  $P$  of a ferroelectric film, the jumps of  $90^\circ$  domain walls over the misfit dislocations represent one of the possible microscopic mechanisms of the *Barkhausen effect* in thin films. On the macroscopic scale, this classical effect manifests itself in pulses of the switching current and multiple steps on the polarization hysteresis loops  $P(E)$ , which are commonly observed in ferroelectrics.<sup>45–48</sup>

To check whether the proposed mechanism is realistic, we have to compare the introduced critical field  $E_{\text{cr}}$  with the measured coercive field  $E_c$  of an epitaxial ferroelectric film with the  $90^\circ$  domain structure. For the discussed representative film/substrate system with the relative coherency strain  $S_r = 1.006S_r^0$ , film thickness  $H = 10H_0$ , and dislocation spacing  $L = 100H_0$ , the calculation gives the critical field of  $E_{\text{cr}} \approx 0.012E_0$  for the first domain jump. This result leads to an estimate  $E_{\text{cr}} \approx 2.5 \times 10^6$  V/m for the  $\text{PbTiO}_3$  film at room temperature, which has the characteristic field  $E_0 \approx 2 \times 10^8$  V/m.<sup>44</sup> Remarkably, the calculated critical field is several times lower than the coercive field  $E_c \approx 10^7$  V/m evaluated from the measured hysteresis loops of epitaxial  $\text{PbTiO}_3$  films.<sup>49</sup> On the other hand, the critical field necessary for a domain jump increases drastically in the film/substrate systems, where the relative coherency strain  $S_r$  differs strongly from all of the threshold strains  $S_r^*$  at the given dislocation periodicity  $L$ , which were discussed in Sec. III. In real epitaxial systems, however, arrays of misfit dislocations are not exactly periodic. In the presence of a distribution of the dislocation spacings, the boundaries of some  $90^\circ$  domains may be situated close to misfit dislocations in the majority of polydomain epitaxial films. Therefore, the jumps of  $90^\circ$  walls over misfit dislocations are expected to be a common mechanism of the Barkhausen effect in ferroelectric thin films.

In view of the above prediction, it is of interest to analyze the dependence of the critical field  $E_{\text{cr}}$  on the film thickness and other relevant parameters. For this purpose, we represent  $E_{\text{cr}}$  as  $E_{\text{cr}} = E_{\text{th}} + \Delta E_{\text{cr}}$ , where  $E_{\text{th}}$  is the threshold field, which equalizes the two minima of the energy  $\Delta U_c^{\text{md}}(l/L)$ , and  $\Delta E_{\text{cr}}$  is the minimum value of the critical field removing the potential barrier. The field  $E_{\text{th}}$  strongly depends on the initial coherency strain  $S_r$  in the film/substrate system, in-

creasing rapidly with the deviation of  $S_r$  from its threshold value  $S_r^*$ , to which the effective parameter  $S_r/S_r^0 - E/E_0$  tends during the rise of external field. The characteristic estimate of  $E_{\text{cr}}$ , therefore, is given by the difference  $\Delta E_{\text{cr}} = E_{\text{cr}} - E_{\text{th}}$ . Our numerical calculations revealed the following main features in the behavior of  $\Delta E_{\text{cr}}$ .

(i) The minimum critical field  $\Delta E_{\text{cr}}$  varies nonmonotonically with the normalized film thickness  $H/H_0$ . In the case of the  $a/c/a$  domain configuration described by the curves shown in Fig. 5, for example, the first jump of the  $90^\circ$  domain wall over the misfit dislocation takes place at  $\Delta E_{\text{cr}} \approx 8 \times 10^{-3}E_0$  in a film with  $H = 10H_0$ ,  $\Delta E_{\text{cr}} \approx 9 \times 10^{-3}E_0$  at  $H = 100H_0$ , and  $\Delta E_{\text{cr}} \approx 1.6 \times 10^{-3}E_0$  at  $H = 500H_0$ . It can be seen that the critical field reduces drastically in very thick films ( $H \gg 100H_0$ ), which may be expected from general considerations. Indeed, the driving force  $F_{\text{driv}}$  acting on a  $90^\circ$  wall in an electric field is directly proportional to the wall area, which gives  $F_{\text{driv}} \sim H$ . The stress field of a straight edge dislocation, which hinders the domain-wall motion, falls with the distance  $r$  from the dislocation as  $r^{-1}$  so that the pinning force weakly depends on the film thickness at large  $H$ . However, the increase of the critical field with decreasing film thickness stops in very thin films ( $H \sim 10H_0$ ) due to the screening of dislocation stresses by the film free surface.

(ii) The critical field  $\Delta E_{\text{cr}}$  reduces with the increase of the dislocation density  $\rho \sim 1/L$  at the film/substrate interface. This feature is caused by the fact that the degree of stress inhomogeneity near the interface lowers, and the stress-induced potential relief smoothens, as the dislocation spacing  $L$  decreases.

(iii) The larger the number of misfit dislocations inside the embedded  $90^\circ$  domain, the smaller the field  $\Delta E_{\text{cr}}$  necessary for the wall jump over the next dislocation. For instance, in a film with the thickness  $H = 100H_0$  and the dislocation spacing  $L = H$ , the “capture” of the sixth dislocation by the  $90^\circ$  domain requires a field which is about three times smaller than the field  $\Delta E_{\text{cr}}$  necessary for the capture of the first misfit dislocation. This trend can be attributed to the enhancement of the sensitivity of equilibrium domain width  $d^*$  to changes of the relative coherency strain, which accompanies the growth of  $d^*(S_r)$  [see Fig. 3(a)]. Indeed, owing to the increase of the derivative  $\partial d^*/\partial S_r$ , the broadening of a wide domain by a given value  $\Delta d \sim L$  can be induced by a much smaller field  $E/E_0$  than in the case of a narrow domain.

(iv) The critical field  $\Delta E_{\text{cr}}$  displays a *hysteretic behavior* in the sense that it depends on the direction in which the  $90^\circ$  wall jumps over the misfit dislocation. This feature can be revealed during a cyclic variation of an applied electric field, which induces the broadening and shrinking of the embedded ferroelectric domain at different stages of the cycle. To illustrate this hysteretic behavior, we shall consider again the  $a/c/a$  domain configuration characterized by the potential relief shown in Fig. 5. We now suppose that the applied electric field starts to decrease after reaching the critical value  $E_{\text{cr}}^{(1)} \approx 0.012E_0$ , which transforms this relief into curve 4. In this situation, the  $c$  domain captures one misfit dislocation at  $E = E_{\text{cr}}^{(1)}$ , and then shrinks due to the increase of the effective parameter  $S_r/S_r^0 - E/E_0$ . When the field intensity

reduces below the value  $E_{\text{th}} \approx 0.004E_0$  (curve 2), the domain tends to shift back to the initial position between two dislocations. However, even at  $E=0$  it cannot return to this position because the backward jump of the  $90^\circ$  wall is impeded by a potential barrier (see curve 1). This jump takes place only after the application of a critical electric field  $E_{\text{cr}}^{(2)} < 0$  in the opposite direction. The calculation shows that the magnitude of  $\Delta E_{\text{cr}}^{(2)} = E_{\text{cr}}^{(2)} - E_{\text{th}}$  equals  $5.5 \times 10^{-2}E_0$ , which is several times larger than the critical field  $\Delta E_{\text{cr}}^{(1)} \approx 8 \times 10^{-3}E_0$  necessary for the forward jump of domain wall. This distinction is caused by a strong asymmetry of the potential relief  $\Delta U_c^{\text{md}}(l/L)$  (see curve 2 in Fig. 5)

## V. CONCLUSION

In epitaxial thin films grown on dissimilar substrates, the formation of the ferroelastic (twin) structure is driven by the mechanical film/substrate interaction. The density of domain walls is expected to grow rapidly just below the phase transition temperature  $T_c$ , and then to stabilize during the further cooling of the film. The fractions of the film volume occupied by dissimilar ferroelastic domains, on the other hand, were observed to change gradually with the decrease of temperature.<sup>4</sup> This process is caused by the variation of the misfit strain with temperature, which alters the energetically most favorable values of domain populations. The adjustment of domain populations to these equilibrium values proceeds via translational movements of domain walls induced by the thermodynamic forces of mainly mechanical origin.<sup>27</sup> Similar limited movements of ferroelastic walls may result from the substrate bending, which offers a simple way to change the misfit strain in an epitaxial system.

In ferroelectric thin films, displacements of domain walls can be also induced by an applied electric field. In contrast to the large-scale motion of purely ferroelectric walls, which is permitted in a constrained film, the displacements of ferroelastic walls under the electric field are very limited. They are restricted by the aforementioned thermodynamic forces, which now play the role of restoring forces. Owing to the elastic stabilization of the  $90^\circ$  domain structure, the contribution of  $90^\circ$  walls to the polarization switching in tetragonal ferroelectric films must be small in comparison with the contribution of  $180^\circ$  walls. Nevertheless, significant changes of the volume fraction  $\phi_c$  of the  $c$  domains have been observed during the polarization reversal in epitaxial  $\text{Pb}(\text{Zr}_{0.32}\text{Ti}_{0.68})\text{O}_3$  thin films.<sup>28</sup>

In the presence of misfit dislocations in an epitaxial film, the movements of ferroelastic walls are hindered by additional potential barriers. When the driving field acting on a

wall becomes strong enough, the wall leaps over the neighboring dislocation. Our theoretical results show that such jumps may manifest themselves in steplike changes of the domain populations, measured as a function of temperature, substrate deformation, or the intensity of applied electric field. Moreover, the ferroelastic domain structure can display a hysteretic behavior under the cyclic variation of a driving field. Therefore, the hysteresis, which was observed in Ref. 28 during x-ray measurements of the electric-field dependence of the  $c$ -domain population  $\phi_c$ , may be attributed to the pinning of  $90^\circ$  walls by misfit dislocations in epitaxial  $\text{Pb}(\text{Zr}_{0.32}\text{Ti}_{0.68})\text{O}_3$  films.

On the microscopic scale, the elastic interaction between domain walls and misfit dislocations may manifest itself in specific mutual positions of these crystal defects. When the Burgers vector  $\mathbf{B}$  of the dislocations is oriented in the film plane, the energetically most favorable configuration corresponds to the position of a misfit dislocation either inside or outside the embedded  $c$  domain, depending on the relative coherency strain  $S_r$  in the epitaxy and the sign of  $B$ . The location of  $90^\circ$  domain walls in a close vicinity of misfit dislocations can occur only under particular conditions in this case (e.g., when a small domain formed between two neighboring dislocations at the transition temperature grows during the film cooling until it is blocked by these defects). In contrast, misfit dislocations with an out-of-plane Burgers vector  $\mathbf{B}$  of appropriate sign create potential wells for the moving  $90^\circ$  boundaries, thus pinning them to specific positions.<sup>30</sup> A similar link-up of the  $90^\circ$  domain walls with interface dislocations has been observed experimentally in a  $\text{BaTiO}_3/\text{LaAlO}_3$  epitaxial system using high-resolution transmission electron microscopy.<sup>17</sup>

Finally, we would like to note that the quantitative results of our theoretical calculations are directly applicable to polydomain films, where distances between the  $90^\circ$  domains of the same type are much larger than the film thickness. For this geometry of the domain structure, the elastic interaction between the embedded  $c$  domains (or between the  $a$  domains) may be neglected because it is strongly reduced due to the screening effect of the film free surface. Accordingly, the influence of misfit dislocations on the statics and dynamics of polydomain configurations may be described in the approximation of a single embedded domain.

## ACKNOWLEDGMENT

The research described in this publication was made possible in part by Grant No. I/75965 from the Volkswagen-Stiftung, Germany.

<sup>1</sup>Y. Tsao, *Materials Fundamentals of Molecular Beam Epitaxy* (Academic, New York, 1993).

<sup>2</sup>J. Matthews and A. E. Blakeslee, *J. Cryst. Growth* **27**, 118 (1974).

<sup>3</sup>A. L. Roitburd, *Phys. Status Solidi A* **37**, 329 (1976).

<sup>4</sup>B. S. Kwak, A. Erbil, B. J. Wilkens, J. D. Budai, M. F. Chisholm, and L. A. Boather, *Phys. Rev. Lett.* **68**, 3733 (1992); B. S. Kwak,

A. Erbil, J. D. Budai, M. F. Chisholm, L. A. Boather, and B. J. Wilkens, *Phys. Rev. B* **49**, 14865 (1994).

<sup>5</sup>Y. Gao, G. Bai, K. L. Merkle, Y. Shi, H. L. M. Chang, Z. Chen, and D. J. Lam, *J. Mater. Res.* **8**, 145 (1993).

<sup>6</sup>A. E. M. De Veirman, J. Timmers, F. J. G. Hakkens, J. F. M. Cillessen, and R. M. Wolf, *Philips J. Res.* **47**, 185 (1993).

- <sup>7</sup>R. Ramesh, T. Sands, and V. G. Keramidias, *Appl. Phys. Lett.* **63**, 731 (1993).
- <sup>8</sup>J. S. Speck, A. Seifert, W. Pompe, and R. Ramesh, *J. Appl. Phys.* **76**, 477 (1994).
- <sup>9</sup>S. Stemmer, S. K. Streiffer, F. Ernst, and M. Rühle, *Philos. Mag. A* **71**, 713 (1995).
- <sup>10</sup>Y. M. Kang, J. K. Ku, and S. Baik, *J. Appl. Phys.* **78**, 2601 (1995).
- <sup>11</sup>C. M. Foster, Z. Li, M. Buckett, D. Miller, P. M. Baldo, L. E. Rehn, G. R. Bai, D. Guo, H. You, and K. L. Merkle, *J. Appl. Phys.* **78**, 2607 (1995).
- <sup>12</sup>S. Kim, S. Hishita, Y. M. Kang, and S. Baik, *J. Appl. Phys.* **78**, 5604 (1995).
- <sup>13</sup>W.-Y. Hsu and R. Raj, *Appl. Phys. Lett.* **67**, 792 (1995).
- <sup>14</sup>C. M. Foster, W. Pompe, A. C. Daykin, and J. S. Speck, *J. Appl. Phys.* **79**, 1405 (1996).
- <sup>15</sup>M. J. Nystrom, B. W. Wessels, J. Chen, and T. J. Marks, *Appl. Phys. Lett.* **68**, 761 (1996).
- <sup>16</sup>V. Gopalan and R. Raj, *Appl. Phys. Lett.* **68**, 1323 (1996).
- <sup>17</sup>Z. R. Dai, Z. L. Wang, X. F. Duan, and J. Zhang, *Appl. Phys. Lett.* **68**, 3093 (1996).
- <sup>18</sup>S. K. Streiffer, C. B. Parker, A. E. Romanov, M. J. Lefevre, L. Zhao, J. S. Speck, W. Pompe, C. M. Foster, and G. R. Bai, *J. Appl. Phys.* **83**, 2742 (1998).
- <sup>19</sup>J. Lettieri, Y. Jia, M. Urbanik, C. I. Weber, J.-P. Maria, D. G. Schlom, H. Li, R. Ramesh, R. Uecker, and P. Reiche, *Appl. Phys. Lett.* **73**, 2923 (1998).
- <sup>20</sup>J. Chen, L. A. Wills, B. W. Wessels, D. L. Shulz, and T. J. Marks, *J. Electron. Mater.* **22**, 701 (1993).
- <sup>21</sup>V. P. Dravid, H. Zhang, L. A. Wills, and B. W. Wessels, *J. Mater. Res.* **9**, 426 (1994).
- <sup>22</sup>S. Stemmer, S. K. Streiffer, F. Ernst, and M. Rühle, *Phys. Status Solidi A* **147**, 135 (1995).
- <sup>23</sup>D. L. Kaiser, M. D. Vaudin, L. D. Rotter, Z. L. Wang, J. P. Cline, C. S. Hwang, R. B. Marinenko, and J. G. Gillen, *Appl. Phys. Lett.* **66**, 2801 (1995).
- <sup>24</sup>H. Xie, Y.-C. Lu, and R. Raj, *J. Appl. Phys.* **79**, 3675 (1996).
- <sup>25</sup>H.-J. Gao, C. L. Chen, B. Rafferty, S. J. Pennycook, G. P. Luo, and C. W. Chu, *Appl. Phys. Lett.* **75**, 2542 (1999).
- <sup>26</sup>J. C. Jiang, Y. Lin, C. L. Chen, C. W. Chu, and E. I. Meletis, *J. Appl. Phys.* **91**, 3188 (2002).
- <sup>27</sup>N. A. Pertsev and A. G. Zembilgotov, *J. Appl. Phys.* **80**, 6401 (1996).
- <sup>28</sup>K. S. Lee, Y. K. Kim, S. Baik, J. Kim, and I. S. Jung, *Appl. Phys. Lett.* **79**, 2444 (2001).
- <sup>29</sup>J. S. Speck and W. Pompe, *J. Appl. Phys.* **76**, 466 (1994).
- <sup>30</sup>A. Yu. Emelyanov and N. A. Pertsev, *Integr. Ferroelectr.* **32**, 343 (2001).
- <sup>31</sup>G. R. Barsch and J. A. Krumhansl, *Phys. Rev. Lett.* **53**, 1069 (1984).
- <sup>32</sup>W. Cao and G. R. Barsch, *Phys. Rev. B* **41**, 4334 (1990).
- <sup>33</sup>W. Cao and L. E. Cross, *Phys. Rev. B* **44**, 5 (1991).
- <sup>34</sup>E. K. H. Salje, *Phase Transitions in Ferroelastic and Co-elastic Crystals* (Cambridge University Press, Cambridge, 1993).
- <sup>35</sup>J. P. Hirth and J. Lothe, *Theory of Dislocations* (McGraw-Hill, New York, 1968).
- <sup>36</sup>A. Yu. Emelyanov, N. A. Pertsev, and E. K. H. Salje, *J. Appl. Phys.* **89**, 1355 (2001).
- <sup>37</sup>J. Sapriel, *Phys. Rev. B* **12**, 5128 (1975).
- <sup>38</sup>N. A. Pertsev, J. Novak, and E. K. H. Salje, *Philos. Mag. A* **80**, 2201 (2000).
- <sup>39</sup>A. K. Head, *Proc. R. Soc. London, Ser. A* **66**, 793 (1953).
- <sup>40</sup>A. Yu. Emelyanov, *Fiz. Tverd. Tela (Leningrad)* **43**, 316 (2001) [*Phys. Solid State* **43**, 329 (2001)].
- <sup>41</sup>N. A. Pertsev, G. Arlt, and A. G. Zembilgotov, *Phys. Rev. Lett.* **76**, 1364 (1996).
- <sup>42</sup>W. Pompe, X. Gong, Z. Suo, and J. S. Speck, *J. Appl. Phys.* **74**, 6012 (1993).
- <sup>43</sup>For  $\text{PbTiO}_3$  films at room temperature, taking  $B \approx a_0 \approx 0.4$  nm,  $S_c^0 - S_a^0 \approx 0.0656$ , and  $H_0 \approx 1.5$  nm (Ref. 27), we obtain  $\beta \approx 4$ . This estimate of the parameter  $\beta$  was used in our numerical calculations.
- <sup>44</sup>N. A. Pertsev and A. Yu. Emelyanov, *Fiz. Tverd. Tela (Leningrad)* **39**, 127 (1997) [*Phys. Solid State* **39**, 109 (1997)].
- <sup>45</sup>R. R. Newton, A. J. Ahearn, and K. G. McKay, *Phys. Rev.* **75**, 103 (1949).
- <sup>46</sup>A. G. Chynoweth, *Phys. Rev.* **110**, 1316 (1958).
- <sup>47</sup>F. Jona and G. Shirane, *Ferroelectric Crystals* (MacMillan, New York, 1962).
- <sup>48</sup>M. E. Lines and A. M. Glass, *Principles and Applications of Ferroelectrics and Related Materials* (Oxford University Press, Oxford, 1977).
- <sup>49</sup>H. Tabata, O. Murata, T. Kawai, S. Kawai, and M. Okuyama, *Appl. Phys. Lett.* **64**, 428 (1994).